

Helical magnetism and structural anomalies in triangular lattice α -SrCr₂O₄

S E Dutton,^{1*} E Climent-Pascual,¹ P W Stephens,² J P Hodges,³ A Huq,³ C L Broholm⁴
and R J Cava.¹

¹ Department of Chemistry, Princeton University, Princeton, New Jersey 08544, USA

² Department of Physics and Astronomy, Stony Brook University, Stony Brook, New York 11794, USA

³ Neutron Scattering Science Division, Oak Ridge National Laboratory, P.O. Box 2008, MS-6475, Oak Ridge, Tennessee 37831, USA

⁴ Department of Physics and Astronomy, The Johns Hopkins University, Bloomberg 345, 3400 North Charles Street, Baltimore, Maryland 21218, USA

* Corresponding author

Email: sdutton@princeton.edu

Abstract. α -SrCr₂O₄ has a triangular planar lattice of d^3 Cr³⁺ made from edge sharing CrO₆ octahedra; the plane shows a very small orthorhombic distortion from hexagonal symmetry. With a Weiss temperature of -596 K and a three-dimensional magnetic ordering temperature of 43 K, the magnetic system is quasi two-dimensional and frustrated. Neutron powder diffraction shows that the ordered state is an incommensurate helical magnet, with an in-plane propagation vector of $\mathbf{k} = (0, 0.3217(8), 0)$. Temperature dependent synchrotron powder diffraction characterization of the structure shows an increase in the inter-plane spacing on cooling below 100 K and an inflection in the cell parameters at the magnetic ordering temperature. These anomalies indicate the presence of a moderate degree of magneto-structural coupling.

PACS numbers: 75.47.Lx, 75.50.Ee, 61.05.cp, 61.05.fm, 71.70.Ej

1. Introduction

Interest in the low temperature structural and magnetic behaviour of materials with triangular lattices arises from the intrinsic geometric magnetic frustration[1] and the resultant delicate balance between competing magnetic phases that can result in novel magnetic order[2-5] or the absence of long-range ordering.[6] Unlike the kagome lattice, a two-dimensional triangular lattice of classical spins has a unique lowest energy state, with the spins arranged at 120° to one another.[7] However the large number of states close in energy to the ground state allow quantum effects and weaker sub-leading interactions to produce a range of different types of magnetism on triangular lattices.[8, 9, 4, 5, 10, 11] Distortions of the ideal triangular lattice can give rise to incommensurate magnetic ordering with a spiral or helical magnetic ground state, as is observed in CuFeO_2 delafossite[10, 11] and $\text{KFe}(\text{MoO}_4)_2$. [4] The exact behaviour of these systems is highly sensitive to the structure of the materials. For example, changing the size of the inter-layer separation in $A\text{Fe}(\text{MoO}_4)_2$ compounds perturbs the magnetism significantly; $\text{RbFe}(\text{MoO}_4)_2$ has the 120° ordering expected for a triangular lattice,[12, 13] while $\text{KFe}(\text{MoO}_4)_2$ forms two distinct magnetic networks.[4, 5]

The structure of $\alpha\text{-SrCr}_2\text{O}_4$ was previously reported,[14] but its magnetic properties have not been characterized. This material has a layered structure with triangular sheets of formula CrO_2 separated by Sr^{2+} in trigonal prismatic co-ordination (Figure 1). At room temperature there is a small distortion in the triangular Cr^{3+} lattice, which occurs as an indirect effect of the rectangular ordering of the Sr^{2+} between the layers; the result is overall orthorhombic symmetry. The magnetic properties of the analogous Ca compound $\alpha\text{-CaCr}_2\text{O}_4$ have recently been reported.[8] In that compound the Cr^{3+} moments form an antiferromagnetic ground state with helical magnetic ordering at 43 K. $\alpha\text{-SrCr}_2\text{O}_4$ and $\alpha\text{-CaCr}_2\text{O}_4$ are part of a family of isostructural compounds that also includes a Ba variant.[15, 14, 16] The larger alkaline earth versions have an expanded crystallographic unit cell, primarily manifesting as an increase in the separation of the CrO_2 layers. As has been reported for $A\text{CrO}_2$ ($A = \text{Li}, \text{Na}$ and K [17]), this change in inter-planar spacing may be expected to result in changes in the magnetic properties. Here we report the characterization of the low temperature behaviour of $\alpha\text{-SrCr}_2\text{O}_4$. As for the Ca analogue, magnetic ordering in $\alpha\text{-SrCr}_2\text{O}_4$ is observed on cooling below 43 K, with an incommensurate propagation vector, $\mathbf{k} = (0, 0.3217(8), 0)$ consistent with helical magnetic ordering similar to that of $\alpha\text{-CaCr}_2\text{O}_4$. Thus the increase in the inter-planar spacing in this system on going from Ca to Sr has minimal effect on the magnetic ordering. With the onset of three-dimensional magnetic ordering, an inflection in the temperature dependence of all three lattice parameters is observed. Further, the perpendicular-to-plane lattice parameter of $\alpha\text{-SrCr}_2\text{O}_4$ shows an anomalous continuous increase on cooling below 100 K, which reflects a slight increase in the puckering of the CrO_2 layers. These structural changes, though they appear to occur without changing the average structure, may help to relieve the magnetic frustration through local magnetostructural coupling.

2. Experimental

Powder samples of α -SrCr₂O₄ were prepared using a ceramic synthesis route. A stoichiometric mixture of SrCO₃ (Sigma Aldrich, 99.9+%) and Cr₂O₃ (Alfa Aesar, 99.97%) was intimately mixed and then pressed into pellets. The pellets were heated at 50 °C h⁻¹ to 1000 °C under a dynamic vacuum of < 10⁻⁵ Torr. After dwelling at 1000 °C for 2 hours, the furnace was turned off and when at room temperature the chamber was filled with Ar. The sample was then heated to 1550 °C for 12 hours. Initial characterisation using a Bruker D8 Focus diffractometer operating with Cu K α radiation and a graphite diffracted beam monochromator indicated the formation of phase pure α -SrCr₂O₄.

Magnetic susceptibility and specific heat measurements were made using a Quantum Design Physical Properties Measurement System (PPMS). Field dependent magnetization (M) measurements at temperatures between 2 and 300 K showed linear behaviour up to $\mu_0H = 9$ T, and therefore a $\mu_0H = 5$ T field was employed for measurement of the magnetic susceptibility, χ , defined as M/H. Temperature dependent magnetization measurements of finely ground α -SrCr₂O₄ were collected between 2 and 300 K after cooling in zero field. Specific heat was measured in zero field from $2 \leq T \leq 300$ K. The pellet for heat capacity was prepared by heating for 12 hours at 1550 °C under a static argon atmosphere in a vacuum furnace.

The temperature dependence of the lattice parameters was measured by synchrotron powder X-ray diffraction (SXRD) at beam line X16C at the National Synchrotron Light Source at Brookhaven National Laboratory. A sample was loaded in a glass capillary, $\phi = 0.3$ mm, and diffraction patterns ($\lambda \sim 0.70$ Å) were collected between 20 and 280 K. To account for possible wavelength drift during the measurements, an internal silicon standard was employed. Rietveld refinement[18] of the structure was carried out using the Topaz-Academic suite of programs.[19] Backgrounds were fitted using a Chebyshev polynomial of the first kind and the peak shape was modeled using a pseudo-Voigt function.

Neutron powder diffraction measurements were carried out at the Spallation Neutron Source (SNS) at Oak Ridge National Laboratory on the POWGEN time of flight diffractometer. The sample was loaded in a vanadium can, $\phi = 8$ mm, and patterns were collected with wavelength centered at 2.132 Å at 100 K, 50 K and 12 K. To explore the evolution of the magnetic peaks as a function of temperature, shorter scans were also collected at several temperatures below T_N . Rietveld refinement was carried out using the Fullprof program.[20] The background was fit using a six coefficient polynomial function and the peak shape was modeled based on a convolution of back to back exponentials with a pseudo-Voigt function with d-space dependencies of the peak shape and positions appropriate for a cold cryogenic moderator. Additional terms to model anisotropic peak broadening as described by Stephens[21] were included in the refinement; this contribution was fixed to be purely Lorentzian, and all of the six terms allowed by the orthorhombic symmetry $Pmmn$ unit cell were refined.

3. Results

Magnetic susceptibility measurements on α -SrCr₂O₄ show an antiferromagnetic-like transition with $T_N \sim 43$ K (Figure 2). Above T_N the magnetic susceptibility obeys the Curie-Weiss law, $\chi - \chi_0 = C/(T - \theta)$, and fits were carried out for $T > 150$ K. Reflecting the two-dimensional and geometrically frustrating triangular arrangement of the Cr³⁺, the Weiss Temperature, $\theta = -596$ K, is large relative to T_N ($f = \theta/|T_N| = 13.9$). The obtained Curie constant, $C = 2.01$ emu Oe⁻¹ mol_{Cr}⁻¹ K⁻¹ and effective magnetic moment, $\mu_{\text{eff}} = 4.01$ μ_B , are slightly higher than might be expected for paramagnetic Cr³⁺ ($C = 1.875$ emu Oe⁻¹ mol_{Cr}⁻¹ K⁻¹, $\mu_{\text{eff}} = 3.87$ μ_B). This can be attributed to the relatively small temperature range over which fitting to the Curie-Weiss law was carried out and the presence of long-range magnetic fluctuations when $T < |\theta|$. The specific heat of α -SrCr₂O₄ is shown in Figure 3. A sharp feature is observed at $T \sim T_N$; no features are observed at higher temperatures. At low temperatures, $T < 20$ K, the specific heat can be modeled using a power law, $C_p = aT^b$, with $b = 2.98(2)$, indicating that three-dimensional magnetic ordering occurs below T_N . The absence of non-magnetic structural analogues of α -SrCr₂O₄ does not allow for a direct deduction of the lattice contribution to the specific heat and so instead the lattice contribution at low temperature, $T < 75$ K was approximated using a Debye model. The calculated change in entropy is shown as an inset in Figure 3. At T_N , the inferred magnetic entropy increases much less than the full magnetic entropy associated with $S = 3/2$ Cr³⁺ ($2R \ln(2S+1) \sim 23$ J K⁻¹ mol⁻¹), indicating the persistence of two-dimensional or short-range ordering above T_N .

The temperature dependence of the lattice parameters of α -SrCr₂O₄ is shown in Figure 4. Throughout the measured temperature range, the c/b ratio remains constant (~ 0.87) and close to the value expected for an ideal hexagonal lattice (for an ideal hexagonal sheet $c/b = \cos 30 = 0.87$). Thus the geometry of the CrO₂ sheets is close to that of an ideal hexagonal layer. At temperatures between 300 and 100 K, the expected decrease in the unit cell parameters is observed on cooling. At $T \sim 100$ K the a parameter, which is the measure of twice the inter-layer spacing, shows an anomalous increase; no anomalous features are observed in the b and c parameters, which characterize the layers. The increase in the inter-layer spacing is however only ~ 0.01 Å, or 0.02%, on cooling from 100 to 12 K, this is much smaller than the in-plane contraction of $\sim 0.12\%$ over the same temperature range, hence the unit cell volume continues to decrease and no negative volume thermal expansion is observed. At $T \sim T_N$ an inflection point in the temperature dependence of all three lattice parameters is observed. In spite of these anomalies in the thermal expansion of α -SrCr₂O₄, no changes in the symmetry are observed in either the X-ray or neutron diffraction data, with the $Pm\bar{m}n$ unit cell previously described by Pausch and Müller-Buschbaum[14] consistent with the diffraction data from 12 K to 300 K.

A fit to the neutron diffraction data collected at 50 K is shown in Figure 5. Structural parameters and bond lengths from refinement of patterns collected at 12, 50 and 100 K are given in Tables 1 and 2.

Consideration of the connectivity of the Cr lattice shows a triangular lattice with only a minor distortion. The distortions are reflected in the displacements of the refined Cr1 position from an ideal hexagonal pseudosymmetry site at $(\frac{1}{2}, \frac{1}{4}, \frac{1}{2})$ and the non-ideal ratio of the in-plane cell parameters. Within the CrO_2 layers, the orthorhombic symmetry allows the Cr1 to move in the c direction while the y co-ordinate is fixed. Further, the site symmetry of Cr1 permits it to move out of the $x = \frac{1}{2}$ plane, at all temperatures this is observed as a slight puckering of the the CrO_2 sheets which increases on cooling. The net result is that both the in-plane and inter-plane Cr-Cr distances are very slightly different (see Table 2). Over the measured temperature range, an inversion of the short and long interactions within individual triangles in the plane occurs. When averaged over the whole sheet these changes do not reflect any significant variation in the structure of the CrO_2 layers.

A broadening of some of the peaks in the neutron diffraction patterns is observed, which is modeled by the refinement of anisotropic strain parameters. These parameters show a small value (< 0.002 a.u.) associated with $h00$ reflections, intermediate values (0.1-0.2 a.u.) for $0k0$, $hk0$, $h0l$ reflections and larger values (0.4-0.6 a.u.) associated with $00l$ and $0kl$ reflections. The strain thus appears to be primarily associated with the c lattice direction. Comparison of the values obtained for $\alpha\text{-SrCr}_2\text{O}_4$ with those obtained from other triangular lattices[22, 23] shows that the anisotropic broadening is relatively small. Almost constant values of the strain parameters are obtained in refinement of the neutron powder diffraction data collected between 12 and 100 K; only the S_{202} and S_{220} parameters show a significant change, decreasing and increasing on cooling respectively. These two values reflect the coupling between one of two directions within the CrO_2 sheets with the perpendicular x -axis and may reflect how the unusual temperature dependence of the a parameter affects the geometry of the CrO_2 layers. Since the strain is primarily associated with the in-plane reflections it is unlikely that stacking faults are the origin of the strain. Strain of this kind has previously been associated with quench strain from a higher temperature structural phase transition.[24] Alternatively the apparent strain may arise from small domains in $\alpha\text{-SrCr}_2\text{O}_4$ with monoclinic or triclinic symmetry which when spatially averaged yield orthorhombic symmetry, such as found in $\text{V}_{1-x}\text{Mo}_x\text{O}_2$ below its metal to insulator transition.[25] Given the strain associated with the orthorhombic structure at low temperatures, it may be that a structural phase transition to an ideal orthorhombic phase occurs above room temperature. At still higher temperatures, the Sr may disorder and a hexagonal symmetry phase may occur. While this has not been reported for any of the ACr_2O_4 materials,[8, 15, 14, 16] structurally related $\beta\text{-SrRh}_2\text{O}_4$ crystallizes in the hexagonal $\overline{\text{P}}62c$ space group,[26] which has the Sr disordered over two sites between the CrO_2 sheets.

On cooling below T_N additional broad peaks are observed in the neutron diffraction pattern, the two most intense close to $d \sim 4.15 \text{ \AA}$ (Figure 6a). The magnetic scattering can be approximately indexed using the propagation vector, $\mathbf{k} \sim (0, \frac{1}{3}, 0)$ and described using the same magnetic model as proposed for $\alpha\text{-CaCr}_2\text{O}_4$. In this model (Figure 6b), the spins are constrained within the ac -plane and form a spiral

arrangement that propagates along the b -direction. Within the layers, the residual moment from each individual triangle is zero when $\mathbf{k} = (0, \frac{1}{3}, 0)$. Adjacent layers are coupled antiferromagnetically. This magnetic model gives a reasonable fit to the data, however the two peaks observed close to $d \sim 4.15 \text{ \AA}$ are poorly modeled (Figure 6a inset). An incommensurate magnetic ordering, with propagation vector $\mathbf{k} \sim (0, 0.3217(8), 0)$ was found to model the data much better. On warming from low temperatures towards T_N , the intensity of the magnetic reflections decreases (Figure 6c) and just below T_N , at 40 K, a magnetic moment of $1.75(4) \mu_B$ is observed; a significant reduction from the $2.34(3) \mu_B$ observed at 12 K. At 50 K no residual intensity from the magnetic phase is observed, and at $d \sim 4.15 \text{ \AA}$ the intensity cannot be distinguished from the background. The broadening of the magnetic Bragg peaks was originally modeled using the same model for anisotropic broadening as in the structural phase however this did not fully account for the peak shape. The microstrain was thus constrained to be the same as for the nuclear phase and the additional broadening modeled using a spherical harmonic expansion consistent with Laue class mmm . The broadening of the peaks in the magnetic phase is thus an indication of a finite magnetic correlation length. No reduction in the width of the magnetic reflections is observed on cooling and thus the magnetic correlation length in the ordered phase remains constant on cooling from 40 K to 12 K, which is 31 K below T_N . Reduced magnetic correlation lengths are commonly observed in two-dimensional magnets as a consequence of weak disorder and often occur despite the specific heat indicating long-range magnetic ordering.[8, 3] Due to the anisotropic strain present in both the magnetic and structural phases it is difficult to approximate the magnetic correlation length by modeling the peaks, especially given the degree of overlap between the two most intense magnetic reflections. However a rough approximation was made by fitting three reflections, two magnetic and one structural, close to $d \sim 4.15 \text{ \AA}$ using a lorentzian peak shape. By constraining the width of the two magnetic reflections to be the same and accounting for instrumental broadening using the peak from the structural phase a magnetic correlation length of $\xi = 400(200) \text{ \AA}$ was obtained.

4. Discussion

Expansion of the lattice parameter describing the inter-layer spacing on cooling is not unique to α - SrCr_2O_4 ; in the related delafossite family, CuMO_2 ($M = \text{Cr, Al, In, La, and Sc}$) negative thermal expansion is observed.[27-29] The delafossites are structurally very similar to α - SrCr_2O_4 , being comprised of sheets of MO_2 interspaced by linearly coordinated Cu^+ . In CuCrO_2 it is a distortion of the CrO_6 octahedra on cooling which causes the expansion of the inter-layer spacing.[27] In the CuMO_2 ($M = \text{Al, In, La, and Sc}$) compounds[28, 29] however, the expansion on cooling is attributed to a softening of a phonon mode which increases the Cu-O bond length. From our low temperature neutron diffraction measurements there is no indication of an increase in the size of the SrO_6 trigonal prism. However a small change in the geometry of the Cr1 octahedra is seen and as the Cr1-O1 bond length increases a concomitant decrease in

the Cr1-O2 interaction is observed. This distortion is associated with an increase in the displacement of the Cr1 position from the ideal $(\frac{1}{2}, \frac{1}{4}, \frac{1}{2})$ hexagonal position on cooling. The distortion also induces an increase in the difference between the two inter-layer Cr1-Cr1 interactions, puckering the CrO₂ sheets. As a result of the distortion there is an increase in the disparity between the inequivalent Cr1-Cr2 interactions, changing the balance of the magnetic interactions within the Cr³⁺ lattice. For isotropic spin Cr³⁺ (d^3) cations, structural distortions due to orbital ordering are not expected and as such this distortion may be driven by the tendency to singlet formation. A spin-Peierls distortion is associated with the structural transition in the ACr₂O₄ spinels[30-32] and has been discussed in relation to CuCrO₂ delafossite.[27] The changes in all three lattice parameters when $T \sim T_N$ support a spin driven structural distortion, however further experiments are required to investigate the relationship between the structure and magnetic ordering in α -SrCr₂O₄. As is typical for spin-driven structural transitions, the distortions are very small and as such are difficult to detect. More detailed, higher resolution, diffraction measurements around T_N could reveal a lowering of the symmetry to a monoclinic or triclinic unit cell in α -SrCr₂O₄. A transition of this kind has been observed in α -NaMnO₂, a highly distorted triangular lattice in which a structural transition from monoclinic to triclinic symmetry at T_N results in commensurate magnetic ordering.[23]

The temperature dependence of the lattice parameters and structure in the related compound α -CaCr₂O₄ on cooling below room temperature have not been reported, it is thus not possible to make a complete comparison to the properties of α -SrCr₂O₄. At room temperature the structures of the two compounds are similar with the most significant difference being the expansion of the unit cell, primarily in the a direction, when Ca is replaced by Sr. The relative increase in the b and c parameters results in a shift in the c/b ratio, from 0.88 for α -CaCr₂O₄[16] to 0.87 α -SrCr₂O₄,[14] indicating that the CrO₂ layers in α -CaCr₂O₄ are more distorted from the ideal hexagonal lattice. Magnetic measurements show very similar behaviour for the two compounds; both order antiferromagnetically, $T_N = 43$ K with helical magnetic ordering, $\mathbf{k} \sim (0, \frac{1}{3}, 0)$. Differences in the behaviour include the presence of possible lower local symmetry in α -SrCr₂O₄ and an increase in the degree of incommensuration of the propagation vector (for α -CaCr₂O₄ $\mathbf{k} = (0, 0.3317, 0)$ [8]). It is possible that these differences are due to differences in the orthorhombicity of the CrO₂ planes in the two compounds, however despite the changes induced by replacing the Ca with the larger Sr cation the magnetic ordering does not appear to differ significantly. Low temperature high resolution electron microscopy or high resolution diffraction may be of interest to resolve the structure of α -SrCr₂O₄.

Acknowledgements

The authors wish to thank T. M. McQueen for helpful discussions. This research was supported by the US Department of Energy, Division of Basic Energy Sciences, Grant DE-FG02-08ER46544. Use of the National Synchrotron Light Source, Brookhaven National Laboratory, was supported by the U.S.

Department of Energy, Office of Science, Office of Basic Energy Sciences, under Contract No. DE-AC02-98CH10886. Use of the Spallation Neutron Source was supported by the Division of Scientific User Facilities, Office of Basic Energy Sciences, US Department of Energy, under contract DE-AC05-00OR22725 with UT-Battelle, LLC.

References

- [1] Collins M F and Petrenko O A 1997 Triangular antiferromagnets *Canadian Journal of Physics* **75** 605-55
- [2] Ji S, Lee S H, Broholm C, Koo T Y, Ratcliff W, Cheong S W and Zschack P 2009 Spin-Lattice Order in Frustrated ZnCr_2O_4 *Physical Review Letters* **103** 037201/1-4
- [3] Nakatsuji S, Nambu Y, Tonomura H, Sakai O, Jonas S, Broholm C, Tsunetsugu H, Qiu Y M and Maeno Y 2005 Spin disorder on a triangular lattice *Science* **309** 1697-700
- [4] Smirnov A I, Svistov L E, Prozorova L A, Zheludev A, Lumsden M D, Ressouche E, Petrenko O A, Nishikawa K, Kimura S, Hagiwara M, Kindo K, Shapiro A Y and Demianets L N 2009 Chiral and Collinear Ordering in a Distorted Triangular Antiferromagnet *Physical Review Letters* **102** 037202-4
- [5] Svistov L E, Smirnov A I, Prozorova L A, Petrenko O A, Shapiro A Y and Dem'yanets L N 2004 On the possible coexistence of spiral and collinear structures in antiferromagnetic $\text{KFe}(\text{MoO}_4)_2$ *Journal of Experimental and Theoretical Physics Letters* **80** 204-7
- [6] Harris M J, Bramwell S T, McMorrow D F, Zeiske T and Godfrey K W 1997 Geometrical Frustration in the Ferromagnetic Pyrochlore $\text{Ho}_2\text{Ti}_2\text{O}_7$ *Physical Review Letters* **79** 2554
- [7] Huse D A and Elser V 1988 Simple Variational Wave Functions for Two-Dimensional Heisenberg Spin-1/2 Antiferromagnets *Physical Review Letters* **60** 2531
- [8] Chapon L C, Manuel P, Damay F, Toledano P, Hardy V and Martin C 2011 Helical magnetic state in the distorted triangular lattice of $\alpha\text{-CaCr}_2\text{O}_4$ *Physical Review B* **83** 024409
- [9] Serrano-Gonzalez H, Bramwell S T, Harris K D M, Kariuki B M, Nixon L, Parkin I P and Ritter C 1998 Magnetic structures of the triangular lattice magnets $\text{AFe}(\text{SO}_4)_2$ ($A = \text{K}, \text{Rb}, \text{Cs}$) *J. Appl. Phys.* **83** 6314-6
- [10] Fishman R S and Okamoto S 2010 Noncollinear magnetic phases of a triangular-lattice antiferromagnet and of doped CuFeO_2 *Physical Review B* **81** 020402
- [11] Nakajima T, Mitsuda S, Kanetsuki S, Tanaka K, Fujii K, Terada N, Soda M, Matsuura M and Hirota K 2008 Electric polarization induced by a proper helical magnetic ordering in a delafossite multiferroic $\text{CuFe}_{1-x}\text{Al}_x\text{O}_2$ *Physical Review B* **77** 052401
- [12] Inami T 2007 Neutron powder diffraction experiments on the layered triangular-lattice antiferromagnets $\text{RbFe}(\text{MoO}_4)_2$ and $\text{CsFe}(\text{SO}_4)_2$ *Journal of Solid State Chemistry* **180** 2075-9
- [13] Svistov L E, Smirnov A I, Prozorova L A, Petrenko O A, Demianets L N and Shapiro A Y 2003 Quasi-two-dimensional antiferromagnet on a triangular lattice $\text{RbFe}(\text{MoO}_4)_2$ *Physical Review B* **67** 9
- [14] Pausch H and Müller-Buschbaum H K 1974 New crystal-structure of general formula $\text{Me}^{2+}\text{M}^{3+2}\text{O}_4 - \text{SrCr}_2\text{O}_4$ *Zeitschrift fuer Anorganische und Allgemeine Chemie* **405** 1-7
- [15] Cuno E and Mueller-Buschbaum H 1988 Compound formation $\text{MO}:\text{M}_2\text{O}_3$. X. On barium chromate (BaCr_2O_4) *Zeitschrift fuer Anorganische und Allgemeine Chemie* **564** 26-30
- [16] Pausch H and Müller-Buschbaum H K 1974 Die Kristallstruktur von $\alpha\text{-CaCr}_2\text{O}_4$ *Zeitschrift fuer Anorganische und Allgemeine Chemie* **405** 113-8
- [17] Soubeyroux J L, Fruchart D, Delmas C and Le Flem G 1979 Neutron powder diffraction studies of two-dimensional magnetic oxides *Journal of Magnetism and Magnetic Materials* **14** 159-62
- [18] Rietveld H M 1969 A profile refinement method for nuclear and magnetic structures *Journal of Applied Crystallography* **2** 65
- [19] Coelho A A 2003 *TOPAS Academic: General Profile and Structure Analysis Software for Powder Diffraction Data* edition 3; Bruker AXS: Karlsruhe, Germany
- [20] Rodríguez-Carvajal J 1993 Recent advances in magnetic structure determination by neutron powder diffraction *Physica B: Condensed Matter* **192** 55-69
- [21] Stephens P W 1999 Phenomenological model of anisotropic peak broadening in powder diffraction *Journal of Applied Crystallography* **32** 281-9
- [22] Damay F, Poienar M, Martin C, Maignan A, Rodríguez-Carvajal J, Andre G and Doumerc J P 2009 Spin-lattice coupling induced phase transition in the $S=2$ frustrated antiferromagnet CuMnO_2 *Physical Review B* **80**

- [23] Giot M, Chapon L C, Androulakis J, Green M A, Radaelli P G and Lappas A 2007 Magnetoelastic coupling and symmetry breaking in the frustrated antiferromagnet alpha-NaMnO₂ *Physical Review Letters* **99** 247211
- [24] Rodriguez-Carvajal J, Fernandez-Diaz M T and Martinez J L 1991 Neutron-diffraction study on structural and magnetic properties of La₂NiO₄ *Journal of Physics-Condensed Matter* **3** 3215-34
- [25] Holman K L, McQueen T M, Williams A J, Klimczuk T, Stephens P W, Zandbergen H W, Xu Q, Ronning F and Cava R J 2009 Insulator to correlated metal transition in V_{1-x}Mo_xO₂ *Physical Review B* **79**
- [26] Hector A L, Levason W and Weller M T 1998 Structure of beta-SrRh₂O₄ from X-ray and neutron powder diffraction *Eur. J. Solid State Inorg. Chem.* **35** 679-87
- [27] Poienar M, Damay F, ccedil, oise, Martin C, Hardy V, Maignan A, Andr, eacute and Gilles 2009 Structural and magnetic properties of CuCr_{1-x}Mg_xO₂ by neutron powder diffraction *Physical Review B* **79** 014412
- [28] Li J, Sleight A W, Jones C Y and Toby B H 2005 Trends in negative thermal expansion behavior for AMO₂ (A=Cu or Ag; M=Al, Sc, In, or La) compounds with the delafossite structure *Journal of Solid State Chemistry* **178** 285-94
- [29] Li J, Yokochi A, Amos T G and Sleight A W 2002 Strong Negative Thermal Expansion along the O-Cu-O Linkage in CuScO₂ *Chemistry of Materials* **14** 2602-6
- [30] Lee S H, Gasparovic G, Broholm C, Matsuda M, Chung J H, Kim Y J, Ueda H, Xu G, Zschack P, Kakurai K, Takagi H, Ratcliff W, Kim T H and Cheong S W 2007 Crystal distortions in geometrically frustrated ACr₂O₄ (A = Zn, Cd) *Journal of Physics: Condensed Matter* **19** 145259/1-4
- [31] Ehrenberg H, Knapp M, Baehz C and Klemme S 2002 Tetragonal low-temperature phase of MgCr₂O₄ *Powder Diffraction* **17** 230-3
- [32] Ortega-San-Martin L, Williams A J, Gordon C D, Klemme S and Attfield J P 2008 Low temperature neutron diffraction study of MgCr₂O₄ spinel *Journal of Physics-Condensed Matter* **20** 104238

Table 1: Structural parameters of α -SrCr₂O₄ from refinement of powder neutron diffraction data at various temperatures. Space group $Pmmn$, $Z = 4$.

α -SrCr ₂ O ₄		100 K	50 K	12 K
$a / \text{\AA}$		11.62750(11)	11.62834(10)	11.63013(9)
$b / \text{\AA}$		5.87560(7)	5.87350(7)	5.87184(6)
$c / \text{\AA}$		5.10292(7)	5.10125(6)	5.10019(5)
$V / \text{\AA}^3$		348.62(1)	348.41(1)	348.29(1)
Sr1	z	0.1411(8)	0.1407(7)	1407(68)
$2b$	$B_{\text{iso}} / \text{\AA}^2$	0.76(8)	0.68(7)	0.65(7)
$\frac{1}{4}, \frac{3}{4}, z$				
Sr2	z	0.4530(7)	0.4525(6)	0.4523(5)
$2a$	$B_{\text{iso}} / \text{\AA}^2$	0.35(8)	0.27(7)	0.24(7)
$\frac{3}{4}, \frac{3}{4}, z$				
Cr1	x	0.5039(4)	0.5046(4)	0.5049(4)
$4f$	z	0.4993(10)	0.4981(9)	0.4975(8)
$x, \frac{1}{4}, z$	$B_{\text{iso}} / \text{\AA}^2$	0.383(11)	0.46(9)	0.40(9)
Cr2	$B_{\text{iso}} / \text{\AA}^2$	0.549(11)	0.45(9)	0.37(9)
$4c$				
$0,0,0$				
O1	x	0.5909(3)	0.5912(3)	0.5910(2)
$4f$	z	0.1627(8)	0.1638(7)	0.1649(6)
$x, \frac{1}{4}, z$	$B_{\text{iso}} / \text{\AA}^2$	0.22(8)	0.26(7)	0.23(7)
O2	x	0.4152(3)	0.4148(2)	0.4143(2)
$4f$	z	0.8231(8)	0.8226(7)	0.8233(6)
$x, \frac{1}{4}, z$	$B_{\text{iso}} / \text{\AA}^2$	0.29(9)	0.34(8)	0.22(7)
O3	x	0.40605(15)	0.40612(13)	0.40617(12)
$8g$	y	0.4997(4)	0.4999(4)	0.4993(4)
x, y, z	z	0.3333(6)	0.3333(6)	0.3337(5)
	$B_{\text{iso}} / \text{\AA}^2$	0.23(6)	0.26(6)	0.21(5)

Table 2: Bond Lengths in α -SrCr₂O₄ at various temperatures obtained from powder neutron diffraction.

α -SrCr ₂ O ₄	100 K	50 K	12 K
Sr1-Sr2 / Å	3.595(3)x2 4.222(4)x2	3.596(2)x2 4.216(3)x2	3.596(2)x2 4.215(3)x2
Sr1-O1 / Å	2.414(5)x2	2.413(4)x2	2.418(3)x2
Sr1-O3 / Å	2.533(3)x4	2.534(3)x4	2.537(2)x4
<Sr1-O> / Å	2.49	2.49	2.50
Sr2-O2 / Å	2.382(4)x2	2.376(3)x2	2.372(3)x2
Sr2-O3 / Å	2.576(3)x4	2.578(3)x4	2.575(2)x4
<Sr2-O> / Å	2.51	2.51	2.51
Cr1-O1 / Å	1.993(6)	1.980(6)	1.970(5)
Cr1-O2 / Å	1.948(6)	1.957(6)	1.967(5)
Cr1-O3 / Å	1.997(4)x2 2.041(4)x2	1.984(4)x2 2.043(4)x2	1.995(4)x2 2.039(4)x2
<Cr1-O> / Å	2.00	2.00	2.00
Cr2-O1 / Å	1.991(3)x2	1.995(2)x2	1.996(2)x2
Cr2-O2 / Å	1.986(3)x2	1.989(2)x2	1.990(2)x2
Cr2-O3 / Å	2.021(3)x2	2.021(2)x2	2.022(2)x2
<Cr2-O> / Å	2.00	2.00	2.00
Cr1-Cr1 (in-plane) / Å	2.939(0)x2	2.939(0)x2	2.938(0)x2
Cr2-Cr2 (in-plane) / Å	2.938(0)x2	2.937(0)x2	2.936(0)x2
Cr1-Cr2 (in-plane) / Å	2.941(4)x2 2.948(4)x2	2.935(4)x2 2.952(4)x2	2.932(4)x2 2.954(4)x2
<Cr-Cr> (in-plane) / Å	2.94	2.94	2.94
Cr1-Cr1 (inter-layer) / Å	5.701(5) 5.929(5)	5.707(7) 5.921(7)	5.723(7) 5.904(7)
Cr2-Cr2 (inter-layer) / Å	5.815(0)x2	5.814(0)x2	5.814(0)x2
<Cr-Cr> (inter-layer) / Å	5.82	5.81	5.81

Figure Captions

Figure 1: (a) Structural model of α -SrCr₂O₄ (b) the projection of the CrO₂ layers onto the bc -plane, the Cr-Cr distances are those obtained from neutron powder diffraction at 50 K and show the very small distortion from an ideal hexagonal lattice. CrO₆ octahedra for the crystallographically distinct Cr1 and Cr2 sites are shown in blue and orange respectively. The Sr²⁺ cations, situated between the CrO₂ layers are light grey.

Figure 2: Magnetic susceptibility (M/H) as a function of temperature for α -SrCr₂O₄. The inverse susceptibility (H/M) is inset.

Figure 3: Specific heat of α -SrCr₂O₄ as a function of temperature. An estimate of the change in magnetic entropy using the Debye model to subtract the lattice entropy, $T < 75$ K, is inset.

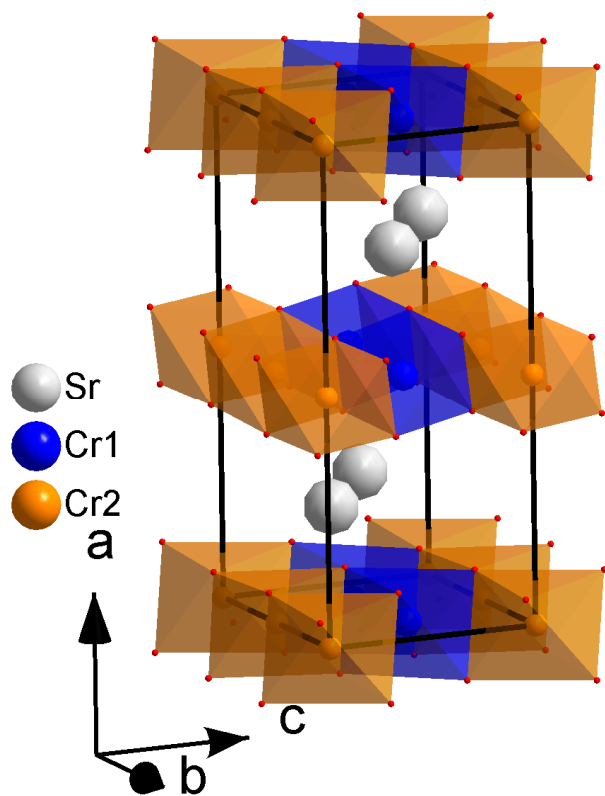
Figure 4: Temperature dependence of the lattice parameters and volume of α -SrCr₂O₄ as determined from synchrotron X-ray diffraction. For an ideal hexagonal bc -plane $b\cos30 = c$. The solid lines are a guide to the eye, unless shown the error bars are smaller than the data points.

Figure 5: Observed (red points) and calculated (black line) neutron diffraction data for α -SrCr₂O₄ collected at 50 K. The difference curve is also shown; reflection positions for the main phase of α -SrCr₂O₄ (upper) and a Cr₂O₃ impurity (0.33(1) wt%) (lower) are indicated by the vertical lines.

Figure 6: (a) Observed (red points) and calculated (black line) neutron diffraction data for α -SrCr₂O₄ collected at 12 K. The difference curve is also shown; reflection positions for the nuclear (upper) and magnetic (middle) phases of α -SrCr₂O₄ and a Cr₂O₃ impurity (0.29(2) wt%) (lower) are indicated by the vertical lines. Fits to the magnetic peak at $d \sim 4.15$ Å for $\mathbf{k} = (0, 0.3217(8), 0)$ (lower) and $\mathbf{k} = (0, 1/3, 0)$ (upper) are shown in more detail in the inset. (b) The magnetic structure of α -SrCr₂O₄. Cr1 and Cr2 atomic sites are shown in blue and orange respectively. (c) The evolution of the magnetic peaks at $d \sim 4.15$ Å as a function of temperature.

Figure 1

(a)



(b)

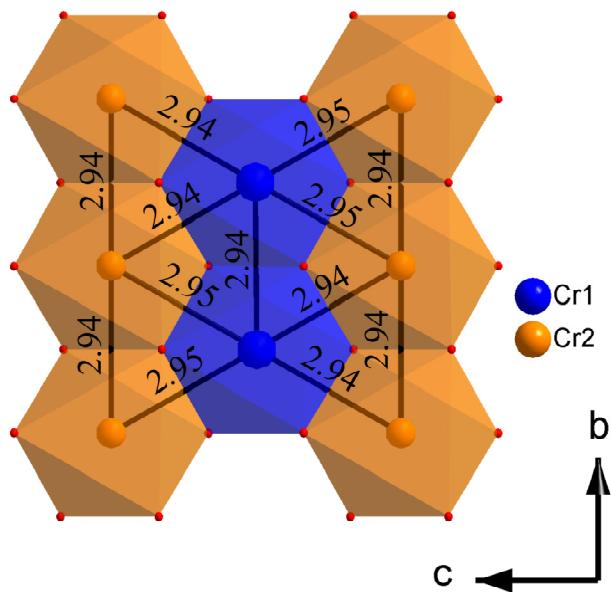


Figure 2

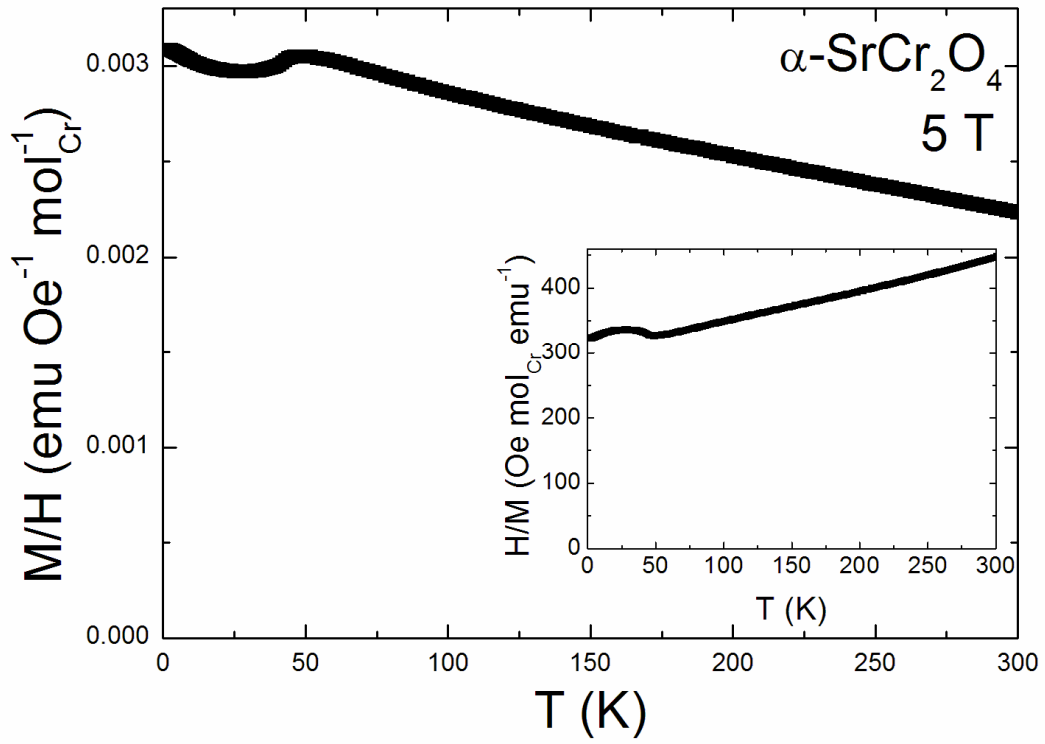


Figure 3

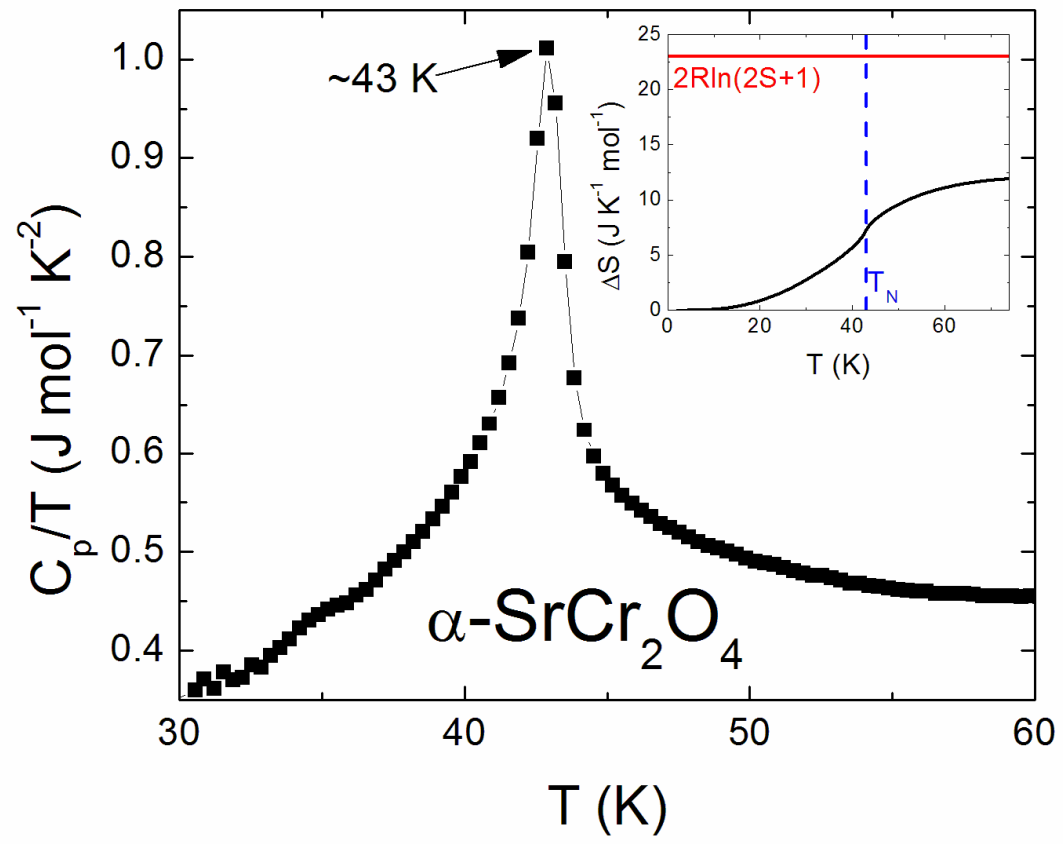


Figure 4

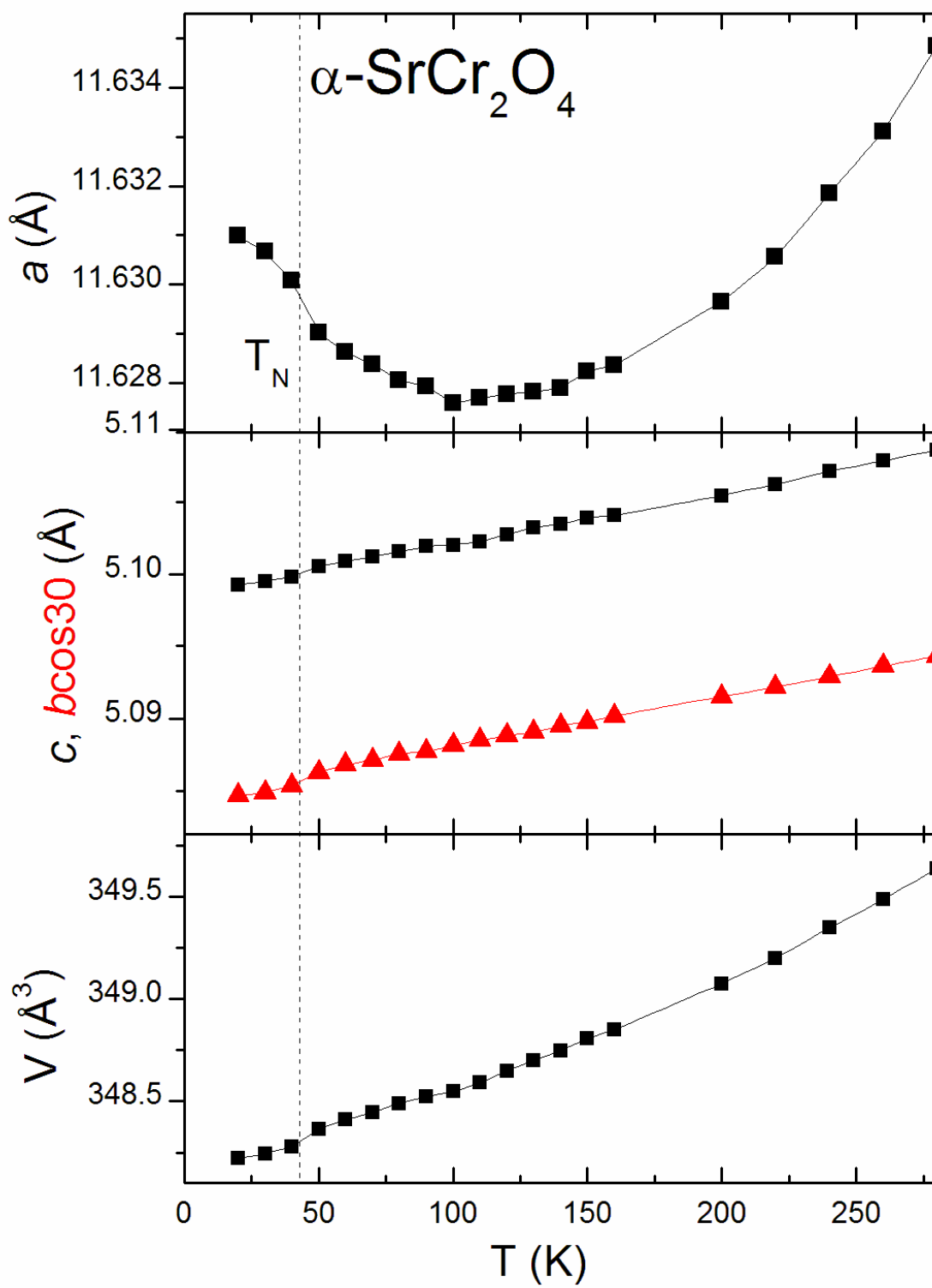


Figure 5

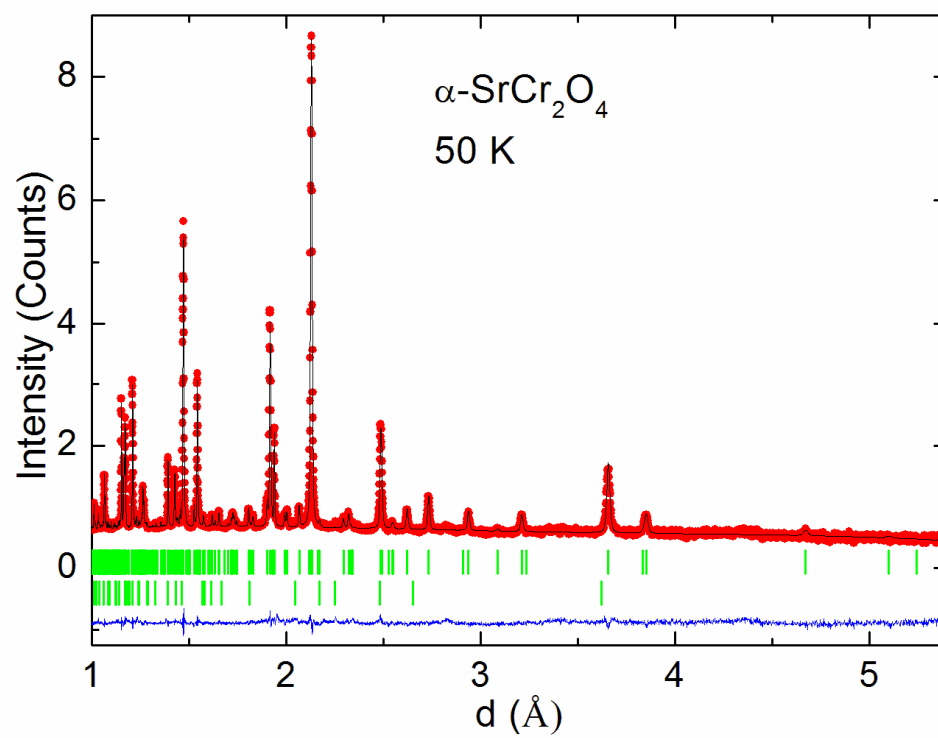


Figure 6

